THE ASTROPHYSICAL JOURNAL, 345:L13–L16, 1989 October 1

WEAK BUMP QUASARS

JONATHAN C. MCDOWELL, MARTIN ELVIS, BELINDA J. WILKES, STEVEN P. WILLNER, M. S. OEY, AND ELISHA POLOMSKI
Harvard-Smithsonian Center for Astrophysics

JILL BECHTOLD
Steward Observatory, University of Arizona

AND

RICHARD F. GREEN
Kitt Peak National Observatory, NOAO[1]

Received 1989 April 25; accepted 1989 July 20

ABSTRACT

The recent emphasis on "big bumps" dominating the ultraviolet continuum of quasars has obscured the fact that bump properties vary widely and that there are objects in which no such component is evident. As part of a survey of quasar continuum spectra, we have identified a class of quasars in which the optical-ultraviolet continuum "big bump" feature appears to be weak or absent, relative to both infrared and X-ray. These "weak bump" quasars are otherwise normal objects and constitute a few percent of the quasar population.

Subject headings: quasars — spectrophotometry — ultraviolet: spectra

I. INTRODUCTION

The ultraviolet "big bump" is the most striking feature in the continuum energy distributions of quasars (Malkan 1983). This bump is part of a larger feature that extends through the optical and, probably, soft X-ray bands (Arnaud *et al.* 1985; Czerny and Elvis 1987). The feature is thought to be a signature of thermal radiation from the accretion flow (which is often modeled as a disk) at a few tens of Schwarzschild radii from the central compact object (Malkan 1983; Bechtold *et al.* 1987, and others). During a study of big bump properties in a sample of quasars with fully observed energy distributions (100 μm–4 keV), we found that in a minority of quasars (five of the 31) the bump appears unusually weak or possibly absent.

II. WEAK BUMP QUASARS

The range of bump strengths in our sample is illustrated in Figure 1 by three quasar energy distributions. The *Einstein* X-ray observations are plotted as a "bow-tie" illustrating the best-fit power law slope and 90% errors (see Wilkes and Elvis 1987, hereafter QED1, for details). Spectrophotometric and photometric observations are plotted as solid lines and individual points, respectively. Optical spectrophotometry is from Neugebauer *et al.* (1979, 1987). *IRAS* AO photometry, near-IR and optical photometry, and *IUE* spectrophotometry are from our QED Atlas—Elvis *et al.* (1989).

The data have been corrected for Galactic reddening and converted to the emitted frame assuming $H_0 = 50$ km s^{-1} Mpc^{-1} and $q_0 = 0.5$; emission lines have been removed and a reddening correction has been made using a standard Galactic extinction law (Savage and Mathis 1979) normalized using small-beam N_H values obtained in the direction of the quasars (Elvis, Lockman, and Wilkes 1989). In cases where substantial variability is evident in the data, an attempt has been made to keep only observations of similar dates. In most of our objects only mild variability is evident.

The object 3C 263 (Fig. 1*a*) has one of the most prominent bumps in our sample, while PG 1116+215 (Fig. 1*b*) is a more typical object; its ultraviolet bump is less pronounced (it does have a large 3000 Å bump caused by Balmer-continuum and unresolved Fe II line emission; Wills, Netzer, and Wills 1985). In contrast, Mrk 876 (Fig. 1*c*) clearly has a much flatter spectrum than the other two objects; it is a "weak bump" quasar. Our sample contains four more "weak bump" quasars, shown in Figure 2, that have no significant rise in their continuum flux toward the far-ultraviolet other than the 3000 Å feature.

While the objects noted as lacking strong ultraviolet bumps by Edelson and Malkan (1986) and Ward *et al.* (1987) were clearly reddened, we will argue that the five objects discussed here are intrinsically weak in the ultraviolet. Properties of the five weak bump quasars are listed in Table 1A. For comparison we list the other quasars from Figure 1, and seven quasars whose energy distributions were published in Elvis *et al.* (1986) and Bechtold *et al.* (1987), in Table 1B. The luminosities of the weak bump quasars are typical of the others in the sample, a few times 10^{45} ergs s^{-1} in the near-infrared, bright enough that contamination due to host galaxy starlight can be ignored. (although Mrk 205 is less luminous, at a few times 10^{44} ergs s^{-1}.) Most of our sample objects, and our five weak bump objects in particular, vary by at most 0.1–0.2 dex (i.e., $\Delta \log L_\nu \sim 0.1$–0.2) based on our observations and those from the literature (Table 1). Variability closer to 0.5 dex would be needed to simulate the weak bump energy distributions.

To define ultraviolet bump strength objectively we use a far-ultraviolet–to–near-infrared color,

$$C_{\rm UV/IR} = \log\left[\frac{L(0.1 - 0.2\ \mu{\rm m})}{L(1 - 2\ \mu{\rm m})}\right].$$

Figure 3 shows the histogram of bump strengths for all quasars in our sample analyzed so far. Despite the near-constant loca-

[1] Operated by the Association of Universities for Research in Astronomy, Inc., under contract with the NSF.

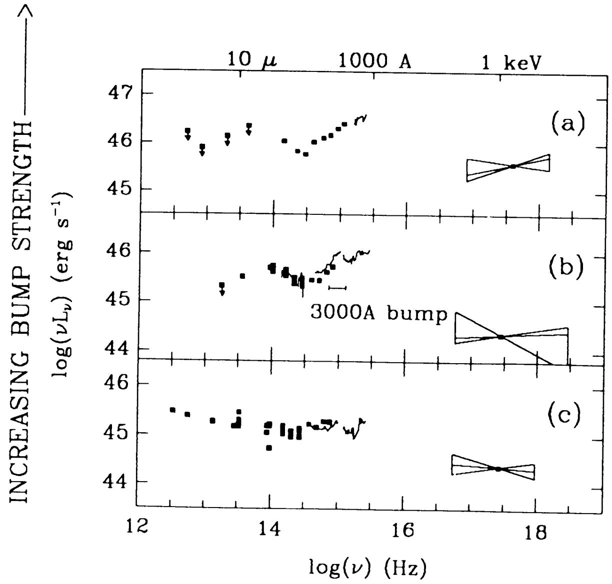

FIG. 1.—Sample rest frame energy distributions for three quasars, illustrating the range of ultraviolet bump strengths. The energy distributions are plotted as log (νL_ν) against log ν; (*a*) 3C 263 has one of the strongest bumps of any of our sample quasars, while (*b*) PG 1116+215 is typical. (*c*) Mrk 205 is a weak bump quasar.

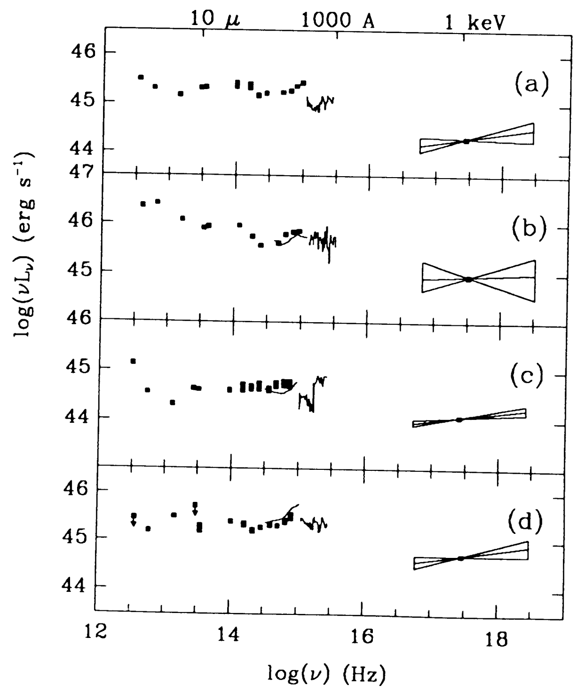

FIG. 2.—Rest frame energy distributions of weak bump quasars: (*a*) PHL 909; (*b*) 3C 48; (*c*) Mrk 205; and (*d*) PHL 1657. Note the presence of the 3000 Å bump at log ν = 14.5–15; it is especially prominent in (*a*) and (*d*).

tion of the 1 μm inflection (Elvis *et al.* 1986), there is a large range in the bump amplitudes. Most of our QED sample objects have strong ultraviolet bumps, with colors bluer than $C_{\mathrm{UV/IR}} = 0.4$ (Table 1B). However there is a tail in the distribution to redder $C_{\mathrm{UV/IR}}$, and those objects picked out visually as having weak bumps are exactly those with $C < 0.15$ (Table 1A).

Could it be that the infrared is enhanced rather than that the ultraviolet is weakened? It seems not. Three-way comparisons among the infrared (1–2 μm), ultraviolet bump, and X-rays show that the weak bump quasars differ from other quasars by being weak in the ultraviolet rather than abnormally strong in the infrared. Also the (far-IR–to–far-UV) luminosities of the quasars range from 10^{45} to 10^{47} ergs s^{-1}, and there is no evidence within this sample for a correlation of bump strength with luminosity.

III. LIMITS ON INTERNAL REDDENING

An obvious possibility is that the range in bump strengths is due to differing amounts of internal reddening in the sources. To test this, we construct color-color diagrams using ratios between the estimated luminosities in various frequency octaves. Figure 4 is an (IR/visible, visible/UV) color-color plot.

TABLE 1

PROPERTIES OF WEAK BUMP QUASARS

Object	Coordinate Name	z	Bump Strength $C_{\mathrm{UV/IR}}$	Observation Date: Near-IR	Observation Date: Optical	Observation Date: *IUE*	Optical Variation (dex)
A. Weak Bump Quasars							
PHL 909	Q0054+144	0.17	−0.20	1985	1978	1987	...
3C 48	Q0134+329	0.37	−0.01	1975	1978, 1985	1982	0.1
Mrk 205	Q1219+755	0.05	0.15	1986	1972, 1986	1983	0.1
Mrk 876	Q1613+658	0.13	0.14	1985	1980, 1985	1981/1983	0.1
PHL 1657	Q2135−147	0.20	0.09	1985	1969, 1985	1982	0.2
B. Other Quasars							
PG 1116+215	Q1116+215	0.18	0.50	1986	1980, 1986	1982	0.2
3C 263	Q1137+660	0.65	0.66	1986	1986	1982	...
PG 1211+143	Q1211+143	0.09	0.56	1986	1980, 1985	1982	0.2
3C 273	Q1226+023	0.16	0.64	Many	1980, 1986	1982	0.3
PG 1307+085	Q1307+085	0.16	0.62	1988	1980, 1986	1980	0.1
PG 1416−129	Q1416−129	0.13	0.59	1988	1980, 1985	1980	0.2
Mrk 1383	Q1426+015	0.09	0.82	1983	1980, 1986	1983	0.2
Mrk 841	Q1501+106	0.04	0.21	1986	1980, 1986	1983	0.2
3C 323.1	Q1545+210	0.27	0.46	1985	1980, 1986	1983	0.1

REFERENCES.—Elvis *et al.* 1986, 1989; Bechtold *et al.* 1987; Neugebauer *et al.* 1979, 1987.

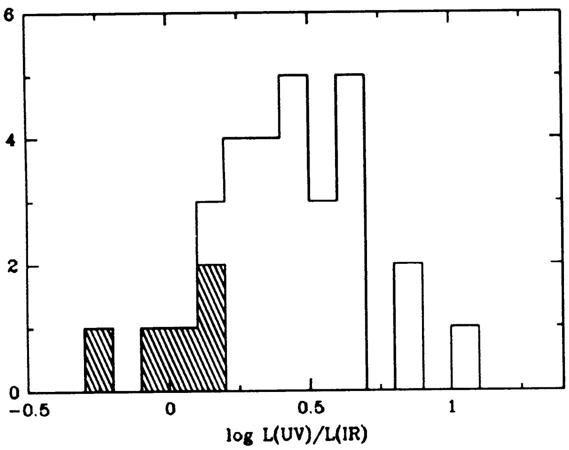

FIG. 3.—Histogram of bump strength colors $C_{IR/UV} = \log L(0.1\text{–}0.2\ \mu m)/L(1\text{–}2\ \mu m)$ for a sample of 30 quasars, including those described in the text. Weak bump quasars are shaded.

As noted earlier, the bump occurs at $\lambda < 1\ \mu m$, so that the ratio of visual (4000–8000 Å) and far-ultraviolet (1000–2000 Å) luminosities largely measures its shape, while the near-infrared (1–2 μm) to visual luminosity ratio measures their "power-law continuum" relative to the bump component. (We avoid the 2000–4000 Å region where the 3000 Å bump is important; Wills, Netzer, and Wills 1985). The reddening lines illustrate that the colors of the weak bump objects could be explained by reddening the "normal" objects by a plausible $E(B-V)$ of 0.1–0.2 mag.

The X-ray data make it unlikely, however, that such strong internal reddening is present. The IPC X-ray spectra for our objects are no different from those of strong bump quasars at the same level of radio loudness (QED1) and are inconsistent with the large hydrogen columns ($> 10^{21}$ cm^{-2}) that would be associated with the internal reddening (0.2 mag) discussed above. For all the weak bump objects, no single power-law X-ray fit with this column is acceptable at the 90% level (see Fig. 2 in QED1). The presence of $E(B-V) = 0.2$ of reddening would imply that the intrinsic spectrum must be curved and extremely steep in the soft X-rays. For instance, for PG 1613+658 the extra intrinsic column density would imply an energy index in the 0.1–4 keV range of $\alpha_E > 2.5$, and neither a single power-law nor a two power-law model gives a good fit to the data if both are absorbed by 10^{21} cm^{-2}. The X-ray column density is unlikely to be smaller than the ultraviolet column since the X-rays are believed to come from a smaller region on energetic grounds. Indeed, there is some evidence that the column to the X-ray–emitting plasma may be greater than toward that emitting at other frequencies (Reichert *et al.* 1985). We therefore conclude that reddening is not likely to be the cause of the bump weakness, unless an extra unabsorbed X-ray component is present (e.g., NGC 4151; Elvis, Briel, and Henry 1983, and Pounds *et al.* 1986).

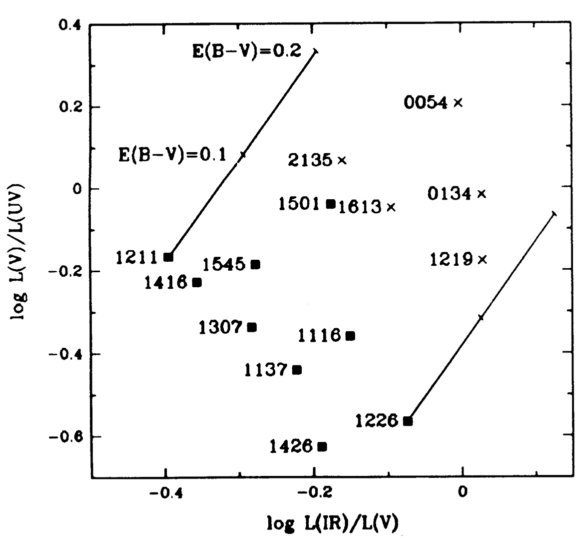

FIG. 4.—Near-infrared/optical/ultraviolet color-color diagram comparing the locus of sample objects with the direction of the reddening line. The lines shows the effect of reddening PG 1211+143 (*center left*) and 3C 273 (*lower right*) by $E(B-V) = 0.1$ and 0.2. Quasars are identified by their right ascensions; weak bump quasars are denoted by crosses, while quasars from Table 1 are represented by filled squares.

IV. DISCUSSION

If reddening is not the dominant effect, there are a number of alternate explanations for the diversity in bump strengths. There does not seem to be any correlation of bump strength with the other main continuum feature, the level of radio loudness, since two of the five weak bump quasars are radio-loud objects. It is possible that the bump may be highly variable in a given object; in this case all quasars may spend some time in the weak bump state, rather than there being a separate class of objects. This would provide strong constraints on parameters for accretion disk models of the bump. While some quasars do vary violently in the ultraviolet (e.g., GQ Comae; Sitko 1986), in the five cases where we have multiple *IUE* observations, the variation is small compared to the range in bump strengths in the sample. Nevertheless, this is a possibility and would be checked by repeated simultaneous optical and ultraviolet observation of the objects in Table 1.

The remaining possibilities require intrinsic differences between the bumps in these objects and those in most quasars. For example, the bump may be present but peak at an abnormally high frequency, in which case its strength would anticorrelate with excesses in the soft X-rays. At present, no quantitative measure of soft excess strength is available, and qualitative comparisons are inconclusive; several weak bump quasars seem to have no soft X-ray excess, but PHL 909, the weakest of all, does show an excess (Masnou *et al.* 1989). Alternatively, the bump may peak at the same frequency but be intrinsically weaker relative to the power-law continuum in these objects, compared to the objects in Table 1B. This could be due either to a true luminosity change or to an inclination effect (cf. Netzer 1985). The range of bump strengths relative to the total luminosity is a factor of 20–50, reasonable for an inclination effect. We note that the expected X-ray behavior with inclination is uncertain, as the central region may become occulted at large inclinations. Finally, the slope of the bump component may be flatter in the weak bump objects. This could occur in accretion disk models if the disks in weak bump quasars were accreting using a different mechanism (with a different geometry?) from those with strong bumps, and had a wider range of contributing temperatures.

If the bump is really absent in some of our objects, what is causing the optical and ultraviolet flux that we do see (especially in the well-observed 0.1–0.5 μm range)? It has been argued (e.g., Sanders *et al.* 1989) that the infrared continuum is entirely due to dust, but dust could not contribute in the optical since the most refractory grains evaporate at around 2000 K. A fairly weak bump and a thermal infrared continuum could conspire to give a continuous infrared-to-ultraviolet power law, but such a coincidence seems contrived. We suggest that the most probable explanation is still that the radiation is nonthermal in origin. The weak bump objects offer new possibilities for studying quasars and may allow us to examine the "bare" nonthermal component in the optical and ultraviolet.

This work was supported by NASA Astrophysics Data Program grant NAG 8-689, NASA *IUE* grant NAG 5-87, and NASA contract NAG 8-30751.

REFERENCES

Arnaud, K. A., *et al.* 1985, *M.N.R.A.S.*, **217**, 105.
Bechtold, J., *et al.* 1987, *Ap. J.*, **314**, 699.
Carleton, N. P., *et al.* 1987, *Ap. J.*, **318**, 595.
Czerny, B., and Elvis, M. 1987, *Ap. J.*, **321**, 305.
Edelson, R., and Malkan, M. A. 1986, *Ap. J.*, **308**, 59.
Elvis, M., *et al.* 1989, "QED Atlas," in preparation.
Elvis, M., Briel, U. G., and Henry, J. P. 1983, *Ap. J.*, **268**, 105.
Elvis, M., Lockman, F. J., and Wilkes, B. J. 1989, *A.J.*, **97**, 777.
Elvis, M., *et al.* 1986, *Ap. J.*, **310**, 291.
Malkan, M. A. 1983, *Ap. J.*, **268**, 582.
Masnou, J-L., *et al.* 1989, in preparation.
Neugebauer, G., Green, R. F., Matthews, K., Schmidt, M., Soifer, B. T., and Bennett, J. 1987, *Ap. J. Suppl.*, **63**, 615.
Neugebauer, G., Oke, J. B., Becklin, E. E., and Matthews, K. 1979, *Ap. J.*, **230**, 79.
Netzer, H. 1985, *M.N.R.A.S.*, **216**, 63.
Pounds, K. A., Warwick, R. S., Culhane, J. L., and de Korte, P. A. J. 1986, *M.N.R.A.S.*, **218**, 685.
Reichert, G., *et al.* 1985, *Ap. J.*, **296**, 69.
Sanders, D. B., Phinney, E. S., Neugebauer, G., Soifer, B. T., Matthews, K., and Green, R. F. 1989, preprint.
Savage, B. D., and Mathis, J. S. 1979, *Ann. Rev. Astr. Ap.*, **17**, 73.
Sitko, M. 1986, in *Continuum Emission in AGN*, ed. M. Sitko (Tucson: NOAO), p. 29.
Ward, M. J., *et al.* 1987, *Ap. J.*, **315**, 74.
Wilkes, B. J., and Elvis, M. 1987, *Ap. J.*, **323**, 243 (QED1).
Wills, B. J., Netzer, H., and Wills, D. 1985, *Ap. J.*, **288**, 94.

JILL BECHTOLD and M. S. OEY: Steward Observatory, The University of Arizona, Tucson, AZ 85721

MARTIN ELVIS, JONATHAN MCDOWELL, BELINDA WILKES, and STEVEN WILLNER: Harvard-Smithsonian Center for Astrophysics, 60 Garden Street, Cambridge, MA 02138

RICHARD GREEN: Kitt Peak National Observatory, NOAO, 950 North Cherry, PO Box 26732, Tucson, AZ 85726

ELISHA POLOMSKI: Department of Astronomy, Boston University, 725 Commonwealth Avenue, Boston, MA 02215